

# Osteoinductive Potential And Bone Healing Capacity Of Nanocrystalline Hydroxyapatite (nHA) Versus Biodentine Of Surgically Created Defects In Rabbits' Alveolar Process (An Animal Study)

Original  
Article

Heba M. Hakam<sup>1</sup>, Rehab A. Abdel Moneim<sup>1,2</sup>, Mona El Deeb<sup>2</sup>

<sup>1</sup>Department of Oral Biology, Faculty of Dentistry, Cairo University, Egypt

<sup>2</sup>Department of Oral Biology, Faculty of Dentistry, Future University, Egypt.

## ABSTRACT

**Background:** Bone defects resulting from trauma, tumor resection, infection, and congenital or acquired deformities remains an important clinical problem. Synthetic nano-crystalline hydroxyapatite, Nano bone, was successfully used in healing of bone defects without revealing negative side effects. Biodentine; a calcium-silicate based material was reported to have osteogenic and angiogenic properties.

**Objectives:** This study aims to investigate the initial osteoinductive potential of Nano Bone and Biodentine on surgically created defects in rabbit's alveolar process.

**Methods:** 30 adult male rabbits (1-1.5kg) were used in this study. Bilateral bone defects were created in the mandibles of all rabbits, one in each side; the right sides were experimental, and the lefts were kept empty as control. Animals were then divided into two groups (15 rabbits each); Group I (Biodentine): The right-side defects were loaded with Biodentine material. Group II (Nano Bone): Nano Bone was packed in the right-side defects. Five rabbits were euthanized from each group at; 3, 7 and 14 days postoperatively. Bone defects' specimens were prepared for histological examination by light microscope as well as quantitative analysis of gene expression of collagen1 alpha and Runx-2 by real time PCR.

**Results:** Biodentine had initiated osteogenesis; yet the newly formed bone was apparently of lesser quality than that formed with Nano Bone. Runx- 2 showed significant increase in Nano Bone compared to Biodentine at 1 week, while collagen1 alpha gene expression was significantly increased at all intervals.

**Conclusion:** Both Nano Bone and Biodentine had initiated osteogenesis. Nano bone showed better healing results when compared to Biodentine.

**Received:** 03 September 2019, **Accepted:** 20 September 2019

**Key Words:** Biodentine, collagen 1 alpha, nano bone, runx-2.

**Corresponding Author:** Heba M. Hakam, MD, Department of Oral Biology, Faculty of Dentistry, Cairo University, Egypt, Tel.: +2 02 5174464, E-mail: hebamhakam@gmail.com

**ISSN:** 1110-0559, xxxxxxxxxxxxxx

## INTRODUCTION

Researchers in the field of regenerative therapy and tissue engineering are always heading for new technologies in cell transplantation, and bioengineering. This quest to develop new techniques and biological substitutes to compensate for damaged tissue<sup>[1]</sup>.

Bone substitute grafts have adventitious characters over autografts and allografts. Bio-mineral morphogenesis is an approach to improve architectural structure of chemicals in micro size and nanocrystal. Hydroxyapatite (HA) is the principal inorganic component of bone and teeth<sup>[1]</sup>. Synthetic HA is widely used in biomedical applications based on its close resemblance to HA structure in bone<sup>[2]</sup>. Nano Bone is an advanced graft material constructed from nanocrystalline hydroxyapatite (nHA). It is a biocompatible candidate applied in many maxillofacial surgeries<sup>[3]</sup>.

Hydroxyapatite ceramics also exhibit minor biodegradation in vivo and proper osteoconductive properties<sup>[2]</sup>. Nano-hydroxyapatite (nHA) was used successfully in sinus floor and alveolar ridge augmentation<sup>[4]</sup>, as well as space-maintenance of bone fractures and intra-bony periodontal defects<sup>[5]</sup>. It was also applied as coating for implants and as a bone filler<sup>[2]</sup>.

Biodentine is a new calcium-silicate based biomaterial that is manufactured using mineral trioxide aggregate (MTA)-based cement technology, which improves its physical properties and handling. Its powder is formed of tricalcium silicate, calcium carbonate and Zirconium oxide for radio-opacity. The liquid consists of calcium chloride, water and polycarboxylate<sup>[6]</sup>.

Biodentine has a short setting time, excellent compressive strength and good sealing properties<sup>[6]</sup>. It is outstandingly

bioactive and biocompatible with the peri-radicular tissues and acquires high physical and chemical qualities in oral environment as in root perforations, apexification, direct pulp capping, retrograde endodontic filling, and in dentin restorative substitution. Few researches highlighted the stimulatory effect of Biodentine on the osteoblastic and periodontal cells' activity and identified it as a bioactive cement<sup>[7]</sup>. The present study aimed to investigate the osteo-inductive potential of Biodentine versus Nano Bone's on surgically created defects in rabbits' mandibular alveolar processes through histological changes as well measuring the levels of the associated proteins Runx-2 and collagen-1-alpha.

## METHODS

### *Ethical statement*

The experiment was held at the animal house, Faculty of Medicine, Cairo University. The design was accepted by Cairo University Institutional Animal Care and Use Committee (CU-IACUC) Medical Science Sector.

### MATERIALS

Nano Bone was supplied as vials containing dry grainy material to be directly packed inside the defect after being mixed with a drop of the animal's blood. According to manufacturer's instructions, mixing the grains with the recipient's blood provides the proteins needed for active bone formation and facilitates regeneration. It is a fully synthetic, granular, biodegradable, biocompatible and highly porous bone grafting material produced by a sol-gel process. It is composed of nanocrystalline, non-sintered hydroxyapatite and silica gel (SiO<sub>2</sub>) up to 76% and 24% respectively. Its particle size is 1.0 x 2.0 mm.

Biodentine was supplied as powder capsules (700mg each) and plastic disposable vials (0.20 ml each). The liquid contains calcium chloride as an accelerator and a hydro soluble polymer that serves as a water reducing agent. Each portion of powder and liquid was mixed according to the manufacturer instruction sheet.

### *Experimental design*

Thirty adult male New Zealand rabbits (1-1.5 kg weight, 31-35 weeks age) were used. Rabbits were housed in the animal house, Faculty of Medicine, Cairo University under veterinarian supervision. Animals were housed separately in stainless steel laboratory rabbit cages under controlled temperature at 25°C ± 2°C with free access to standard unstiffened diet and freshwater inverted plastic flasks.

### *Surgical protocol*

Under sterile conditions, the surgical procedures were performed under general anesthesia with a combination of ketamine hydrochloride (0.08 mL/100g bw) and Xylazine hydrochloride (0.04 mL/100 g bw)<sup>[8]</sup>.

The gingiva was incised over the crest of the ridge in the diastema extent between the incisor and the posterior teeth, then the mucoperiosteum was elevated exposing the bone

surface. A bone defect was fabricated using trephine bur (3mm diameter and 3mm depth) at low-speed hand piece under constant saline irrigation to prevent overheating of bone margins<sup>[9]</sup>. To control the defect size; a fixed size of a surgical bur was used with marking the required length using an endodontic file rubber stopper to provide a fixed depth.

At the end of the surgical procedure, the mucoperiosteum was sutured with 5-0 silk suture (Ethicon®, Johnson and Johnson, São José dos Campos, Brazil). Animals were kept under systemic antibiotic coverage 1 mg/kg once daily for five days postoperatively. Pain was controlled by oral administration of Paracetamol (200 mg/kg, twice a day for 2 days). The surgical procedure was applied on both sides (right and left); where the right-side defect was considered as experimental and the left-side defect was kept empty and set as control.

### *Rabbits were divided into two groups (15 rabbits each)*

**Group I (Biodentine):** The mandibular right-side defects were loaded with Biodentine material.

**Group II (Nano Bone):** The mandibular right-side defects were loaded with Nano Bone material.

Powder and liquid components of Biodentine were manually mixed in parallel by a stainless-steel spatula on a clean glass slab. The paste was then loaded in the defect using a dental composite applicator instrument and then compressed into the defect using an amalgam condenser to secure complete filling of the defect to the level of the surrounding bone surface. Nano Bone was handled in the same manner by mixing its grains with blood drops and loaded as well into the defect.

After the experiment was carried out, animals of both groups were euthanized by intra-cardiac overdoses of sodium thiopental at; 3, 7 and 14 days. At each period, five rabbits were sacrificed from each group. Bone defects' specimens were prepared for histological examination by light microscope as well as for quantitative analysis of gene expression of collagen1 alpha and Runx-2 by real time PCR.

### *Histopathological Examination*

Specimens from each group were soaked in 10% ethylene diamine tetra-acetic acid (EDTA) for 4 weeks to decalcify. Then dehydrated in alcohol, cleared in xylol and embedded in paraffin. Sections of 4-5µ thickness were mounted on regular glass slides and stained by Hematoxylin and Eosin (H and E) for routine histological examination according to the conventional method.

### *Quantitative analysis of gene expression of collagen1 alpha and Runx-2 by real time PCR:*

#### *Total RNA extraction*

Total RNA was extracted according to manufacturer instructions using SV Total RNA isolation system. (Promega,

Madison, WI, USA). The RNA concentrations and purity were measured with an ultraviolet spectrophotometer.

**Complementary DNA (cDNA) synthesis**

The cDNA was synthesized from 1 µg RNA using SuperScript III First-Strand Synthesis System as described in the manufacturer’s protocol (#K1621, Fermentas, Waltham, MA, USA).

**Real-time quantitative PCR (RT-PCR)**

RT-PCR amplification was done with Applied Biosystem with software version 3.1 (StepOne™, USA). The reaction includes SYBR Green Master Mix and gene-specific primer pairs (Table 1). It was designed by Gene Runner Software (Hasting Software, Inc., Hasting, NY) from RNA sequences of the gene bank. Every set of primers exhibited 60° annealing temperature. RT-PCR was done in 25-µl reaction volume formed of 2X SYBR Green PCR Master Mix, 900 nM of every primer plus 2µl of complementary DNA. Amplification was applied under specific time and temperature conditions of several cycles of denaturation and annealing/extension. v1.7 sequence detection software from PE Biosystems (Foster City, CA) was used to calculate the records of RT assays. Comparative Ct technique was used to determine the relative expression of mRNA gene. Data were standardized to beta actin which is the control housekeeping gene.

**Table 1:** Showing the primer sequence of the studied gene

	Primer sequence
Collagen 1 alpha	Forward primer :5'- TCACCTACAGCACGCTTG-3 Reverse primer 5'- GGTCTGTTTCCAGGGTTG -3'
Runx-2	Forward primer :5- GACTGTGGTTACCGTCATGGC -3 Reverse primer: 5- ACTTGGTTTTTCATAACAGCGGA -3
Beta actin	Forward primer :5' --GGTCGGTGTGAACGGATTTGG -3 Reverse primer:5'- ATGTAGGCCATGAGGTCCACC-3

**Statistical analysis**

Statistical analysis was done by the statistical package SPSS version 22. Mean and standard deviation were used to summarize the obtained data. Comparisons between groups were done using analysis of variance (ANOVA) with multiple comparisons post hoc test when comparing more than 2 groups. Correlations between quantitative variables were done using Pearson correlation coefficient<sup>[10]</sup>.

**RESULTS**

**Histological Results**

**I- Three days interval**

**a) Control**

The experimental defects appeared with well-defined open margins. The granulation tissue almost filling the entire defect was infiltrated peripherally with collagen fibers varying from loosely arranged to densely packed. In some areas, the fibers assumed a network entrapping inflammatory cells that were numerous in some areas

with deeply stained, and sometimes, bilobed nuclei. Interconnected bone trabeculae with intervening marrow spaces were detected surrounding the defects margins. (Figure 1)

**b) Biodentine group**

The defects were nearly empty with no evidence of granulation tissue or inflammatory cells, except for tiny collagen bundles which were accidentally found. Scattered remnants of the material were seen inside the defect. In some locations, the material exhibited tight attachment to the bone surface leaving no space intervening. Old bone fragments were obvious together with the regular spongy bone bordering the margins of the defects. (Figure 2)

**c) Nano Bone group**

The defects were apparently empty; but evidence of initial granulation tissue formation could be detected near the base of the specimens. Densely packed fine collagen fibers, inflammatory cells infiltration and congested capillaries were observed among the fibrous tissues. Remnants of the nano material were still detected within the defects. The nano material was observed interlacing with the granulation tissue and infiltrating the nearby marrow cavities. Few osteoclasts were seen scattered within the adjacent marrow spaces of old bone (Figure 3).

**II- One week interval**

**a) Control**

Wide areas of granulation tissue were still obvious with irregularly arranged collagen fibers and heavy inflammatory cells infiltration in relation to the control of the previous interval. Thus, signs of fibrous tissue organization as an early step of osteogenesis could be detected through the onset of confluence of fibrous tissue and emergence of high cellularity filling most of the defect area. Some of these cells were spindle shaped; others appeared with deeply stained basophilic eccentric nuclei. Few blood vessels were seen scattered within the tissue. Sporadic osteoclasts were detected on original bone boundaries of the defect.

Bone trabecular formation started as thin highly cellular septa spreading from and connecting the original bone and dispersed into the granulation tissue. The newly formed trabeculae appeared with different staining intensity than older bone trabeculae. Numerous resting lines were seen within the newly formed bone, the osteocytes lacunae appeared widened and few were empty. The osteocytes’ nuclei exhibited variable sizes and staining intensity (Figure 4).

**b) Biodentine group**

Compared to the control side; greater number of inflammatory cells was detected within the granulation tissue which exhibited densely packed collagen bundles. Inflammatory cells’ condensation was evident within the

defects with multiple multinucleated giant cells near an area assumed to belong to the remains of the used material. Obvious areas of fatty degeneration were detected throughout the defect. Extravasated blood could be seen dispersed within the defects. Scattered trabeculae of woven bone with entrapped osteocytes in wide lacunae were evident. Sometimes, multiple nuclei were seen in separate lacunae with variable shapes and staining intensity. No obvious resting lines were detected (Figure 5)

### **c) Nano Bone group**

Still granulation tissue with densely packed collagen bundles and inflammatory infiltration was obvious but to a fairly lesser extent when compared to the Biodentine group. Areas of woven bone formation were detected with entrapped osteocytes; closely resembling those of the control but lacking resting lines. The newly formed bone covered a greater area of the defects compared to the Biodentine group (Figure 6)

## **III- Two weeks interval**

### **a) Control**

The margins of the defects were not yet approximated. Radiating delicate bone trabeculae were detected within the granulation tissue; some were interconnected enclosing tissues simulating marrow cavities. The newly formed trabeculae revealed entrapped osteocytes and were obviously bordered by osteoblasts. Intertwining with the trabeculae there were areas of fibrous tissue with spindle-shaped fibroblasts. Evidence of inflammatory cells with bilobed nuclei; others assumed large size with multinucleation (Figure 7).

### **b) Biodentine group**

In contrast to control, numerous inflammatory cells infiltrate was still obvious within the defects with bundles of thick collagen fibers. Multinucleated giant cells with spindle shaped cells were detected within the dense fibrous tissue. More bony spicules were revealed than the same group of the previous interval. The entrapped osteocytes appeared with hyperchromatic, pleomorphic nuclei and exhibited widened lacunae; some appeared empty. Osteoblasts like cells were obvious in the vicinity of the newly formed trabeculae in an attempt to line their borders (Figure 8)

### **c) Nano Bone group**

Well defined bone trabeculae within the defects were obvious with embedded osteocytes and were lined along their periphery by osteoblasts. Osteocytes appeared with deeply stained basophilic nuclei in uniform lacunae; yet some appeared empty. Reversal lines together with irregularly arranged numerous resting lines could be detected. Granulation tissue with collagen fibers ranging from widely dispersed to densely packed collagen bundles;

as well as numerous inflammatory cells were seen (Figure 9)

## **Statistical Results**

### **Runx-2**

Statistically significant increase in Runx- 2 gene expression was noted in Biodentine and Nano Bone groups compared to control throughout the three periods ( $p$  value<0.001). No significant difference was detected between Biodentine and Nano Bone groups at 3 days ( $p$  value 0.72) and 2 weeks ( $p$  value 0.45). At 1 week there was a significant increase in Nano Bone group compared to Biodentine ( $p$  value<0.001) (Table 2 a, b, c and Figure 10).

Control specimens showed no significant difference ( $p$  value>0.05) among the three intervals. No significant difference was noted between 1 week and 3 days ( $p$  value 0.9) in Biodentine group. While, there was a significant increase in Runx-2 gene expression in 2 weeks compared to 3 days ( $p$  value<0.001) as well as to 1 week duration ( $p$  value = 0.002). Nano Bone group revealed statistically significant increase in Runx-2 in 1 and 2 weeks compared to 3 days ( $p$  value<0.001); with no difference between 1 and 2 weeks durations ( $p$  value 0.9) (Figure 11)

### **Collagen 1 alpha**

Similar to Runx-2 gene expression; a statistically significant increase in collagen 1 alpha gene expression was detected in Biodentine and Nano Bone groups compared to control ( $p$  value<0.001) through the three periods. At 3 days, a significant increase in collagen1 alpha was noted in Nano Bone group compared to Biodentine ( $p$  value = 0.001). At 1 and 2 weeks; still a statistically significant increase in gene expression was detected ( $p$  value<0.001) (Table 3 a, b, c and Figure 12).

No significant difference was detected in the control specimens throughout the experiment intervals ( $p$  value>0.05). Regarding Biodentine group, no significant difference was noted in collagen 1 alpha between 1 week and 3 days ( $p$  value 0.18); however, there was a significant increase in 2 weeks compared to 3 days ( $p$  value<0.001) as well as to 1 week duration ( $p$  value = 0.019). In the Nano Bone group, there was a significant increase in collagen 1 alpha in 1 and 2 weeks compared to 3 days ( $p$  value 0.019, <0.001 respectively) with no significant difference between 1 and 2 weeks ( $p$  value 0.057) (Figure 13).

### **Correlation between Runx-2 and Collagen 1alpha**

The correlation between collagen 1 alpha and Runx-2 was a very good positive correlation ( $r=0.879$ ,  $p$  value<0.001) where  $r$  = correlation coefficient and  $r > 0.75$ : very good correlation (Figure 14).

**Table 2a:** Showing Runx- 2 gene expression between groups at 3 days interval

	Mean	Std. Deviation	Minimum	Maximum	<i>P1 value</i>	<i>P2 value</i>
Control	.99	.113	.80	1.10	C	
Biodentine	4.92	.77	3.80	5.90	<0.001	C
Nano Bone	5.18	.509	4.70	6.01	<0.001	0.72

**Table 2b:** Showing Runx- 2 gene expression between groups at 1 week interval

	Mean	Std. Deviation	Minimum	Maximum	<i>P1 value</i>	<i>P2 value</i>
Control	1.22	.18	1.03	1.50	C	
Biodentine	5.25	.66	4.50	6.20	<0.001	C
Nano Bone	7.29	.61	6.50	8.07	<0.001	<0.001

**Table 2c:** Showing Runx- 2 gene expression between groups at 2 weeks interval

	Mean	Std. Deviation	Minimum	Maximum	<i>P1 value</i>	<i>P2 value</i>
Control	1.85	.25	1.50	2.10	C	
Biodentine	7.16	1.12	6.10	8.90	<0.001	C
Nano Bone	7.84	.95	6.90	9.20	<0.001	0.45

**Table 3a:** Showing collagen 1 alpha gene expression between groups at 3 days interval

	Mean	Std. Deviation	Minimum	Maximum	<i>P1 value</i>	<i>P2 value</i>
Control	1.24	.37	1.02	1.90	C	
Biodentine	2.59	.51	2.07	3.20	<0.014	C
Nano Bone	4.6	.89	3.40	5.60	<0.001	0.001

**Table 3b:** Showing collagen 1 alpha gene expression between groups at 1 week interval

	Mean	Std. Deviation	Minimum	Maximum	<i>P1 value</i>	<i>P2 value</i>
Control	1.32	.54	.90	2.20	C	
Biodentine	3.63	.59	2.80	4.30	<0.001	C
Nano Bone	6.01	.56	5.20	6.70	<0.001	<0.001

**Table 3c:** Showing collagen 1 alpha gene expression between groups at 2 weeks interval

	Mean	Std. Deviation	Minimum	Maximum	<i>P1 value</i>	<i>P2 value</i>
Control	1.94	.57	1.01	2.50	C	
Biodentine	5.04	.74	4.02	6.01	<0.001	C
Nano Bone	7.26	.51	6.70	8.01	<0.001	<0.001

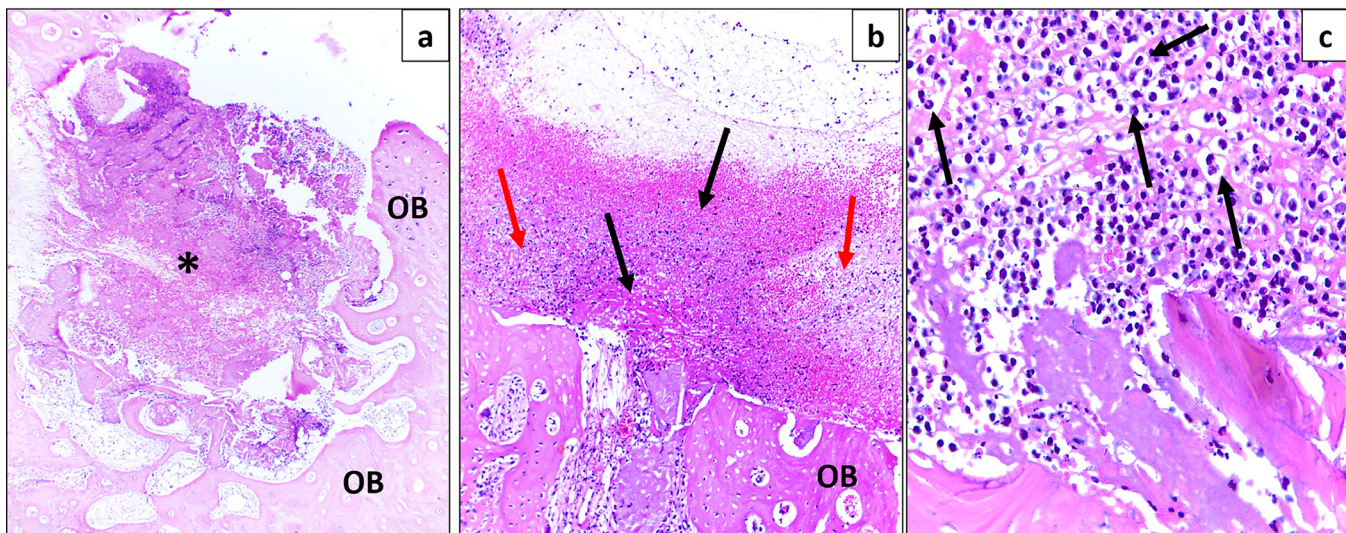


**Fig.1:** Photomicrograph of control (3 days) showing;  
a) Granulation tissue filling the defect (asterisk), old bone (OB) (H&E, Orig.Mag.40X)  
b) Collagen fibers; loosely arranged (red arrow) and densely packed (black arrow), old bone (OB) (H&E, Orig.Mag.100X)  
c) Higher magnification showing; deeply stained inflammatory cells; some assumed bilobed nuclei (arrows) (H&E, Orig.Mag.400X)

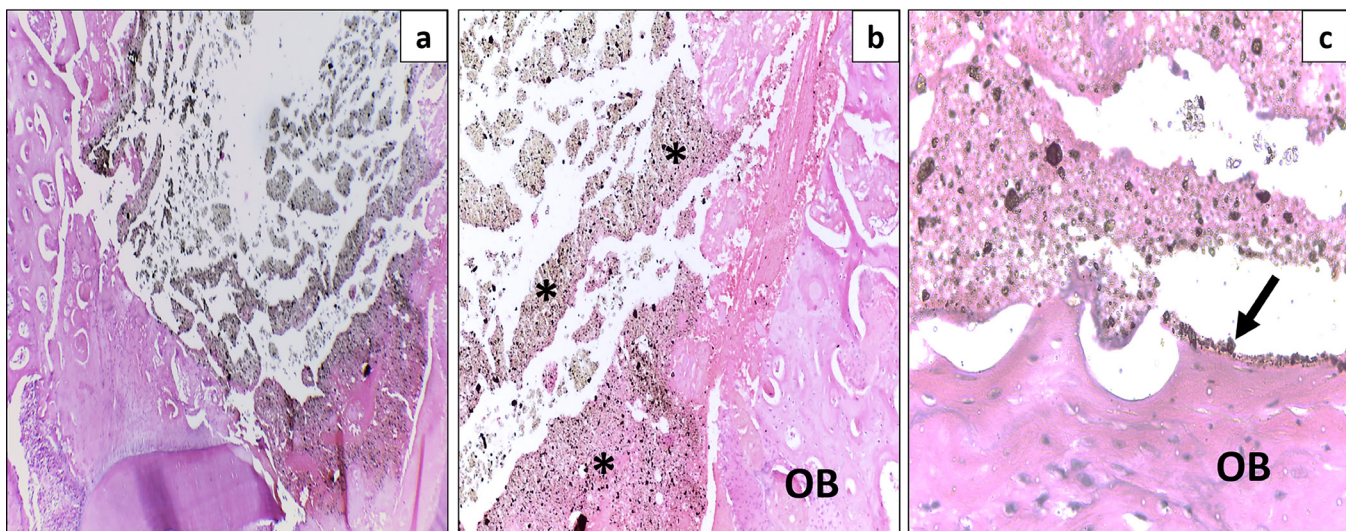


**Fig.2:** Photomicrograph of Biodentine group (3 days) showing;  
a) No granulation tissue or inflammatory cells (H&E, Orig.Mag.40X)  
b) Remnants of the material (asterisks) & old bone (OB) (H&E, Orig.Mag.100X)  
c) Higher magnification showing; tight attachment of the material to bone (arrow) (H&E, Orig.Mag.400X)

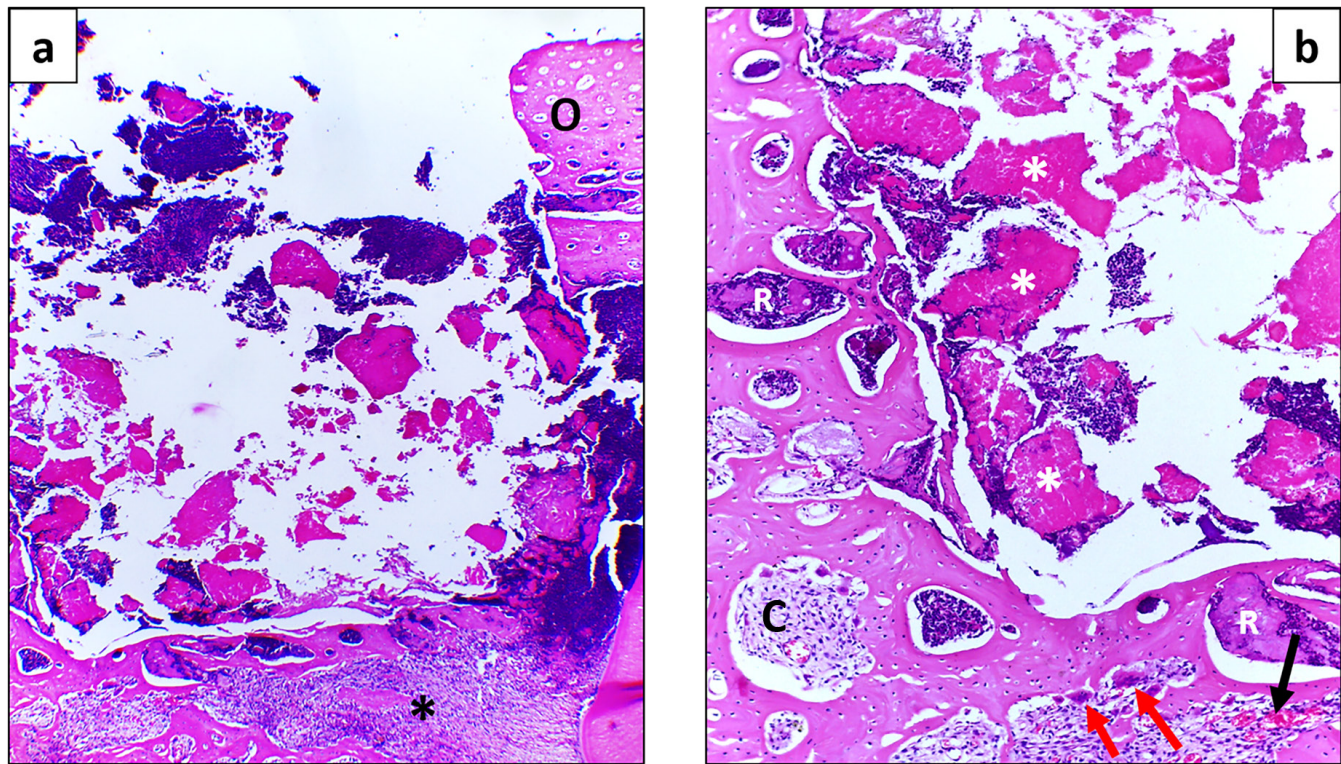


**Fig. 3:** Photomicrograph of Nano Bone group (3 days) showing;  
a) Initial granulation tissue (asterisk) & old bone (O) (H&E, Orig.Mag.40X)  
b) Higher magnification showing; remnants of the nano material within the defects (asterisks) and inside marrow cavities (R), collagen fibers with inflammatory cells (c), congested capillaries (black arrow), few osteoclasts (red arrow). (H&E, Orig.Mag.100X)

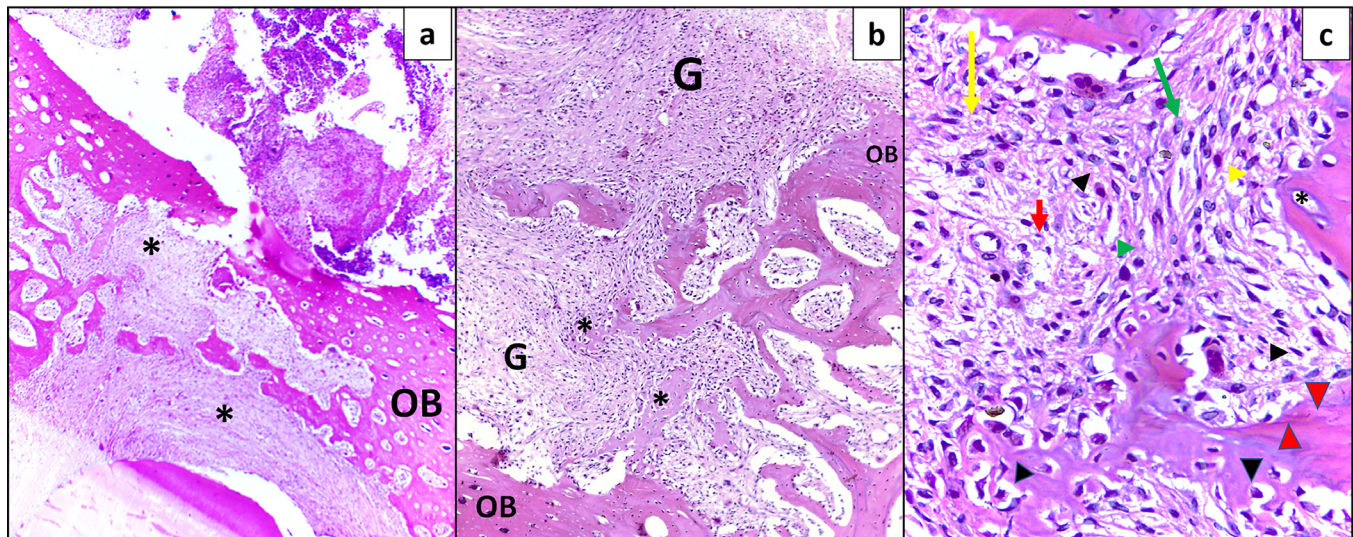


**Fig. 4:** Photomicrograph of control (1 week) showing;  
a) Granulation tissue (asterisks),old bone (OB) (H&E,Orig.Mag.40X)  
b) Highly cellular Fibrous tissue(G), thin highly cellular bony septa (asterisks), original bone (OB) there was a difference in bone stainability between old and new bone (H&E, Orig.Mag.100X)  
c) Higher magnification showing; spindle shaped cells (yellow arrows), cells with eccentric nuclei (green arrows), few blood vessels (red arrow). Widened (black arrowheads) or empty osteocytic lacunae (asterisks) & resting lines(red arrowheads). (H&E, Orig.Mag.400X)

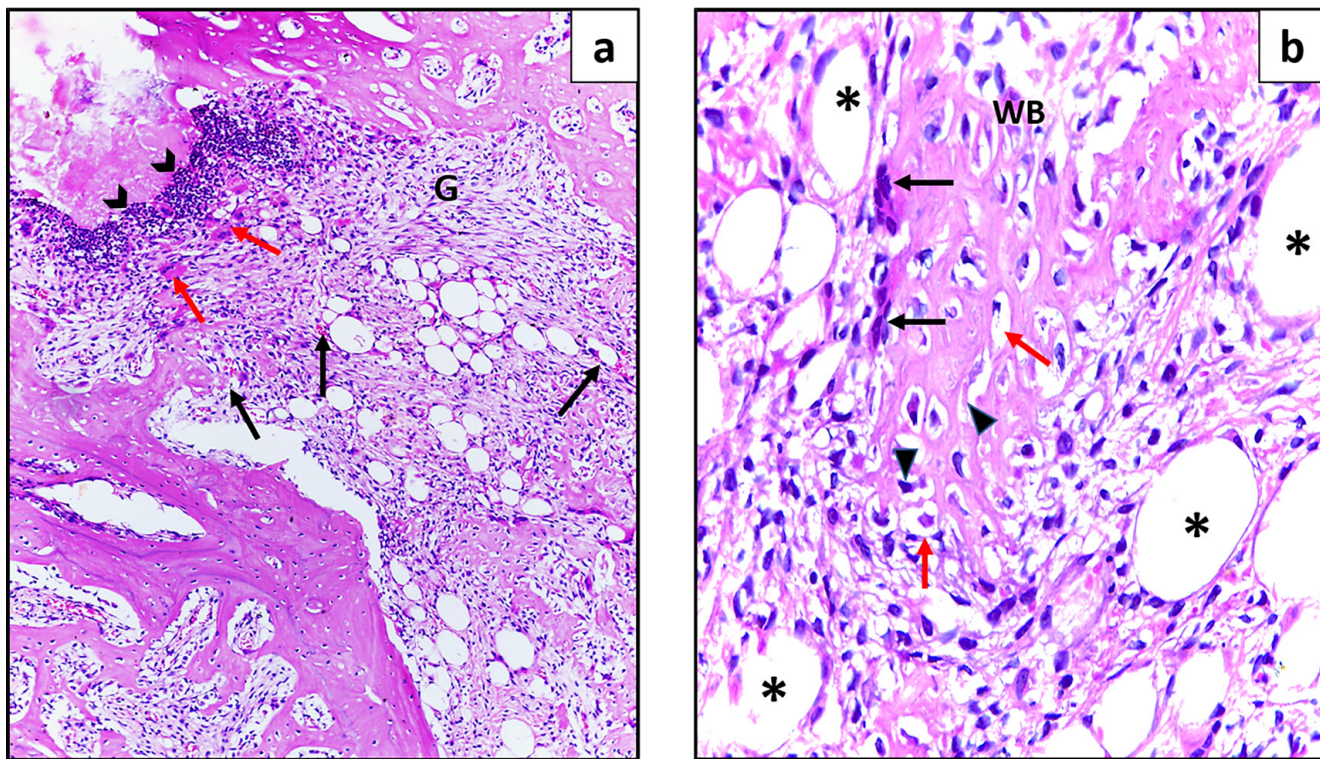


**Fig. 5:** Photomicrograph of Biodentine group (1 week) showing;  
 a) Granulation tissue with inflammatory cells (arrow heads), collagen bundles and fatty degeneration (G), multinucleated giant cells (red arrows), extravasated blood (black arrows) (H&E, Orig.Mag.40X)  
 b) Higher magnification showing; fatty degeneration (asterisks), multinucleated giant cells (black arrows), woven bone (WB) with osteocytes in wide lacunae (red arrows), multiple nuclei in lacunae with variable shapes and staining intensity (arrowheads) (H&E, Orig.Mag.100X)

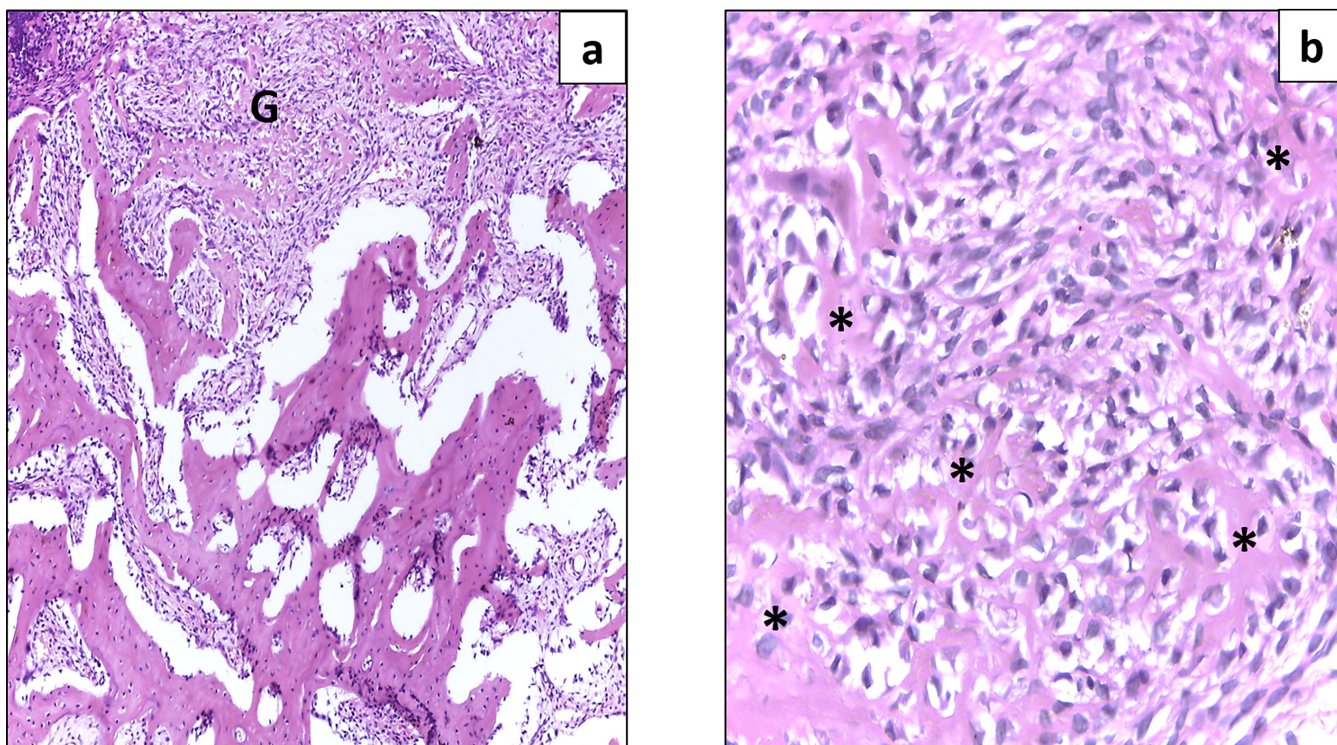


**Fig.6:** Photomicrograph of Nano Bone group (1 week) showing;  
 a) Granulation tissue (G), (H&E, Orig.Mag.40X)  
 b) Woven bone with osteocytes (asterisks) (H&E, Orig.Mag.100X)

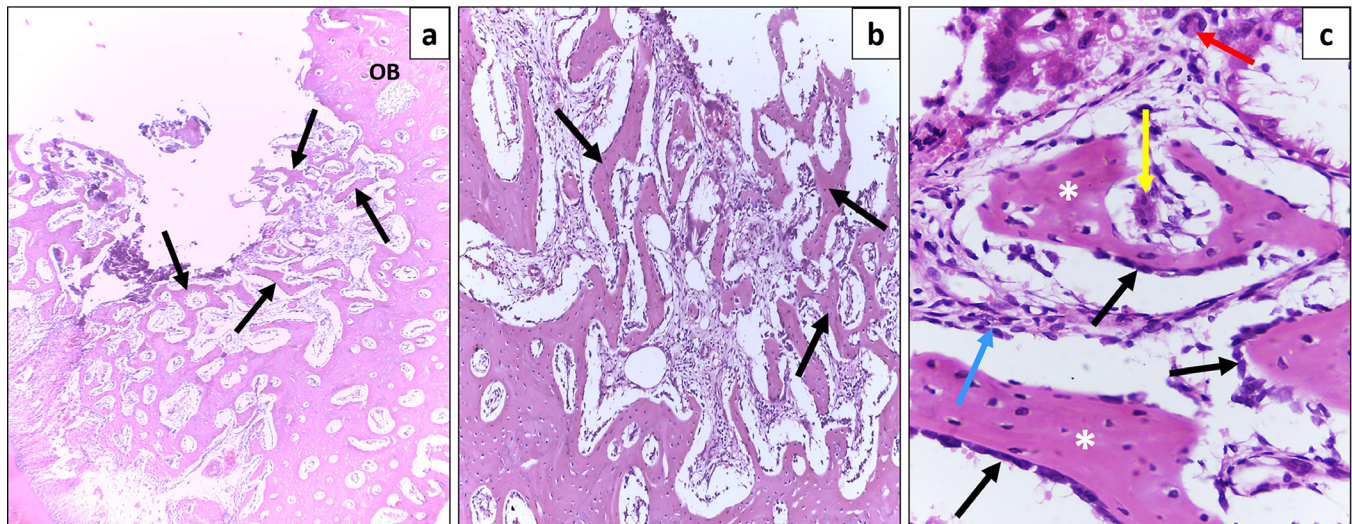


**Fig. 7:** Photomicrograph of control (2 weeks) showing;  
a) Delicate bone trabeculae(arrows), old bone(OB) (H&E, Orig.Mag.40X)  
b) Bone trabeculae enclosing marrow spaces (arrows) (H&E, Orig.Mag.100X)  
c) Newly formed trabeculae bordered by osteoblasts(black arrows), entrapped osteocytes(asterisks), areas of fibrous tissue with spindle-shaped fibroblasts(blue arrow), inflammatory cells with bilobed nuclei(red arrow); others with multinucleation(yellow arrow) (H&E, Orig.Mag.400X)

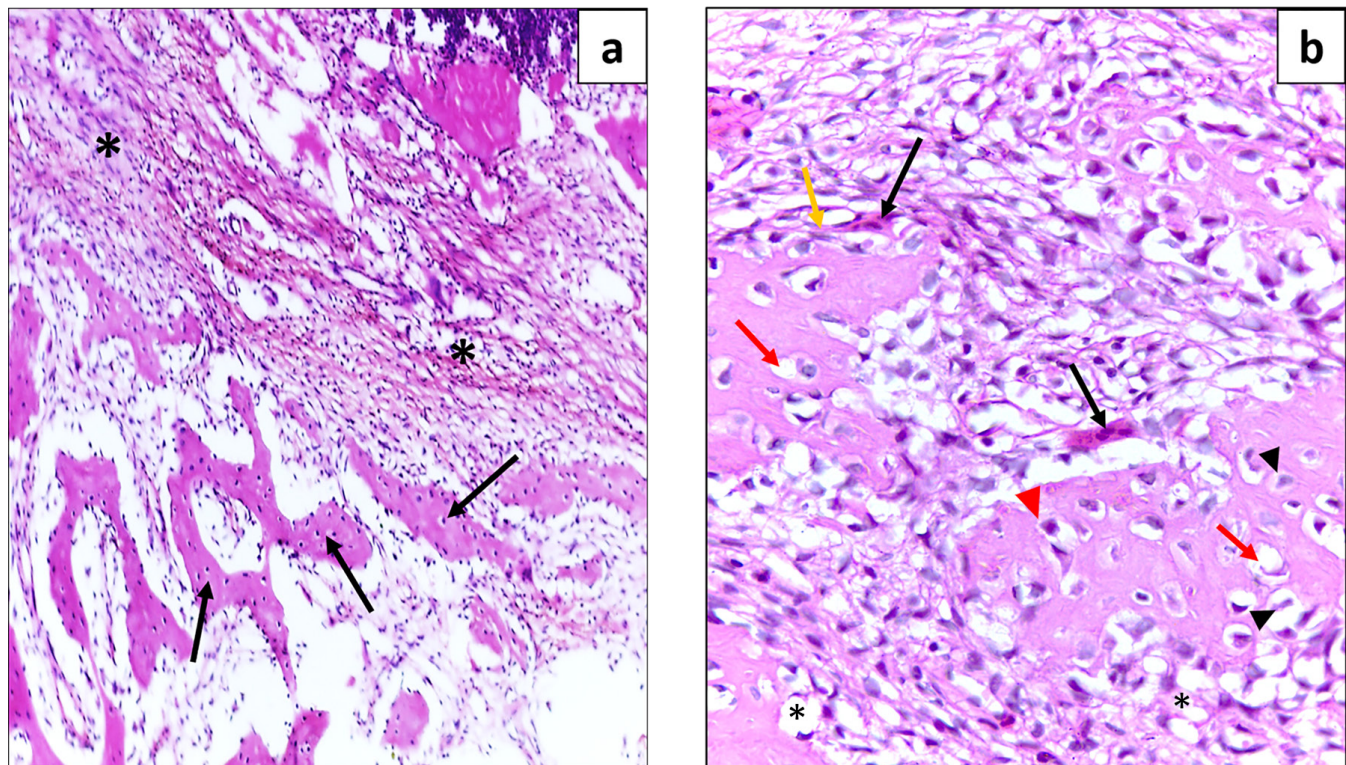


**Fig. 8:** Photomicrograph of Biodentine group (2 weeks) showing;  
a) Inflammatory cells infiltrate with collagen bundles (asterisks),bony spicules (arrows) (H&E, Orig.Mag.40X)  
b) Fibrous tissue with multinucleated giant cells (black arrows), entrapped osteocytes with hyperchromatic (red arrowhead), pleomorphic nuclei (black arrowhead), widened (red arrows) or empty lacunae (asterisk),osteoblasts like cells (yellow arrow) (H&E, Orig.Mag.100X)

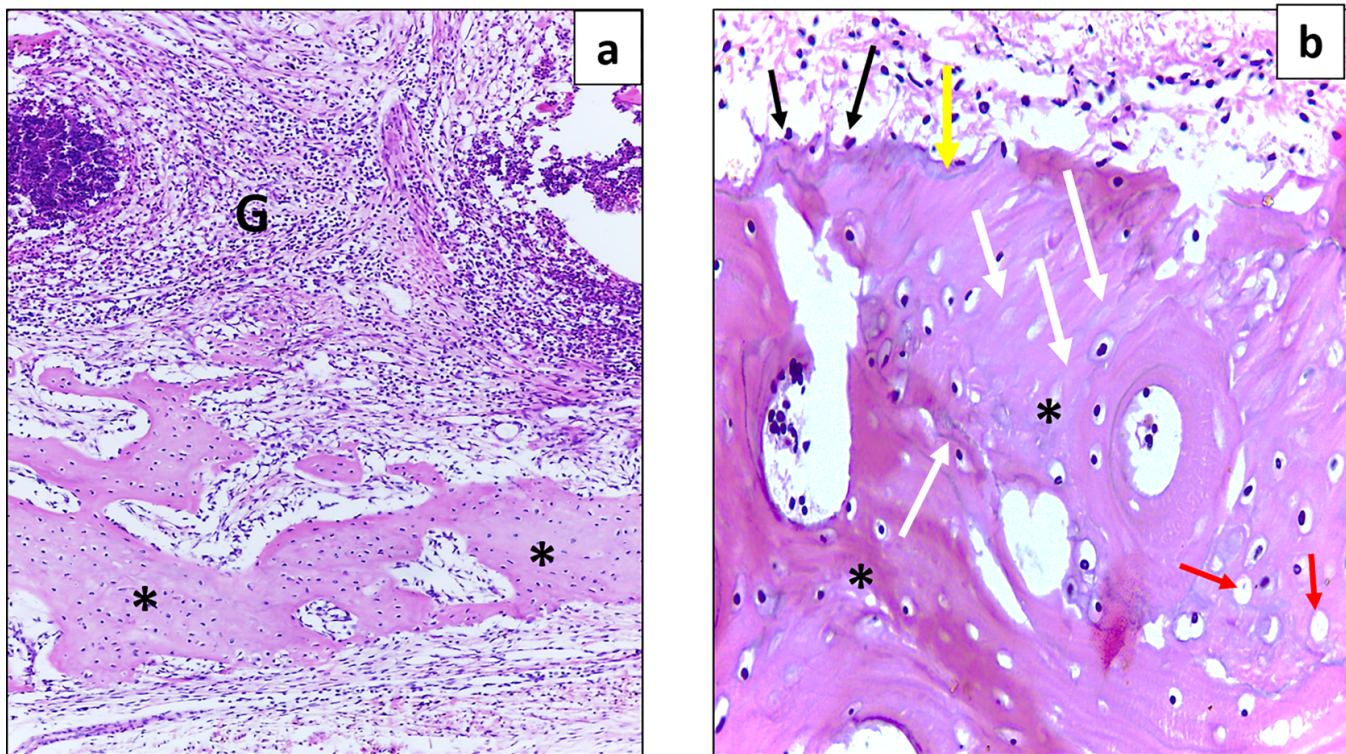


**Fig.9:** Photomicrograph of Nano Bone group (2 weeks) showing:  
 a) Granulation tissue with inflammatory cells and collagen bundles (G),bone trabeculae(asterisks) (H&E, Orig.Mag.40X)  
 b) Higher magnification showing; bone trabeculae lined by osteoblasts(black arrows), with embedded osteocytes in lacunae(asterisks), some appeared empty (red arrows), reversal lines(yellow arrow), resting lines (white arrows) (H&E, Orig.Mag.100X)

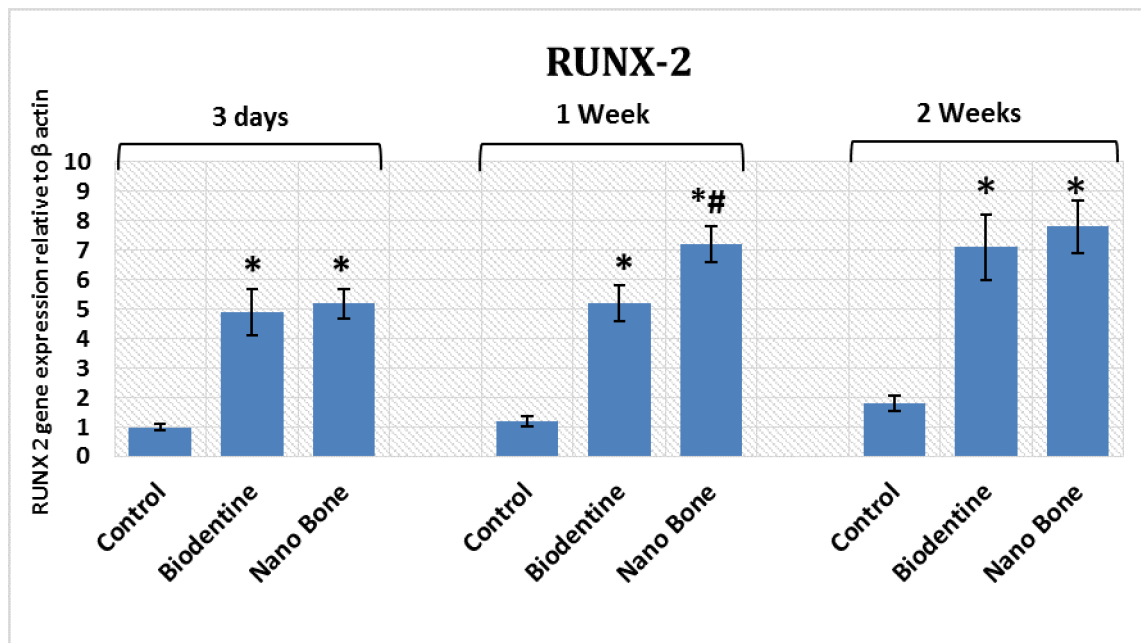


**Fig.10:** Bar chart showing Runx-2 gene expression.  
 (\*) Statistically significant versus control  
 (#) Statistically significant versus Biodentine group

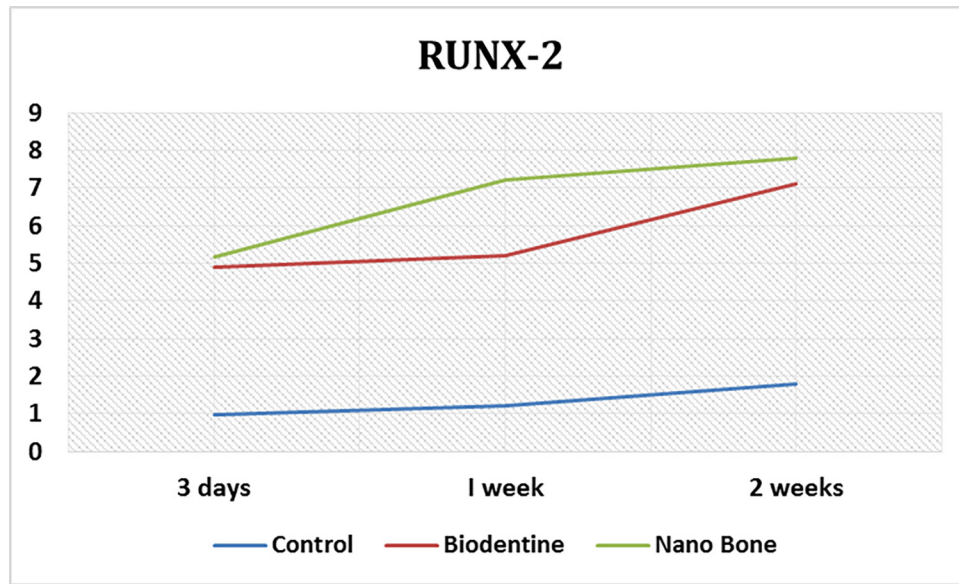


Fig. 11: showing comparison between groups in relation to Runx-2 gene expression.

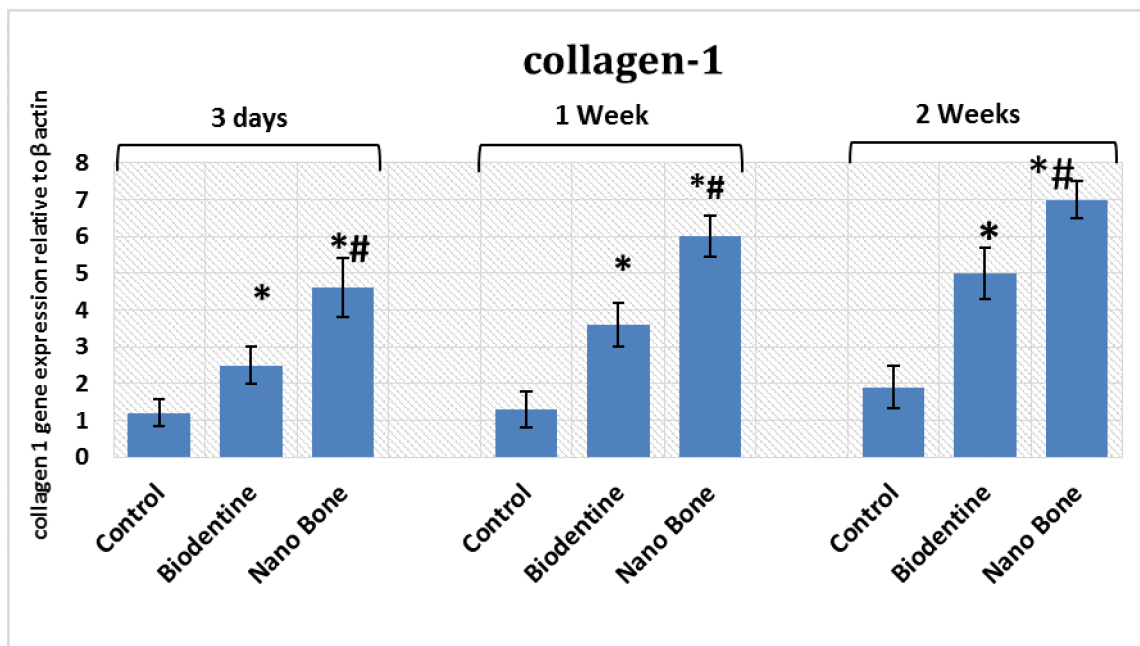


Fig.12: Bar chart showing collagen 1 alpha gene expression.  
 (\*) Statistically significant versus control  
 (#) Statistically significant versus Biodentine group

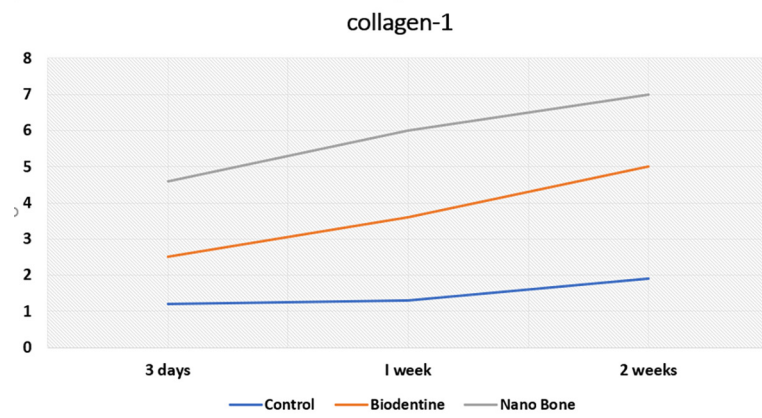


Fig. 13: showing comparison between groups in relation to collagen 1 alpha gene expression.

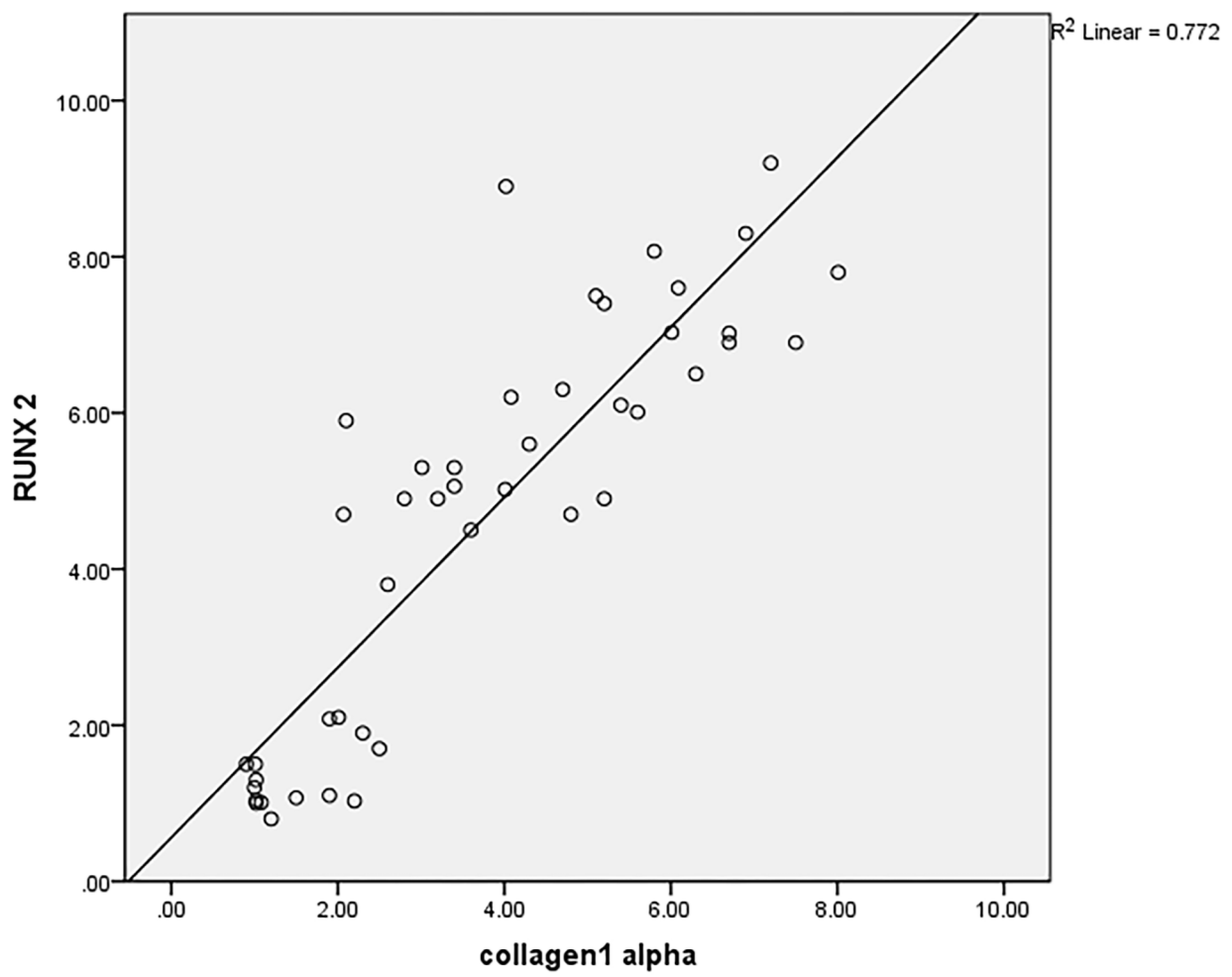


Fig. 14: showing the correlation between collagen 1 alpha and Runx-2.

## DISCUSSION

To evaluate the early osteogenic potential of Nano Bone and Biodentine on surgically created defects in the alveolar process, rabbit was a suitable model for the current research. It is broadly used to examine the osteo-inductive reactions to implants with a rapid postoperative recovery as well as the close resemblance in bone structure between human and rabbit<sup>[11]</sup>.

The studied experimental intervals were selected to concentrate on the aim of monitoring the early events in the healing process as this in our opinion are the most critical events affecting further progress in healing.

Nano-hydroxyapatite (nHA) possesses unique properties related to its small size and large surface area<sup>[1]</sup>. Biomaterial researches have focused on the use of nanotechnology in order to enhance bioreactivity. Thus, bone grafts of synthetic nHA crystals are widely utilized in the repair of bony defects<sup>[2]</sup>.

In our study, Nano Bone group revealed granulation tissue formation with densely packed collagen fibers and inflammatory cells infiltration throughout the three experimental periods. Areas of woven bone formation occupying wide area of the experimental defects were detected in one-week specimens. Bone formation progressed in two weeks samples; showing well defined trabecular bone lined by osteoblasts within the defects, where most osteocytes appeared with deeply stained basophilic nuclei in uniform lacunae. In accordance, significant decrease in pockets' depth was marked in nHA treated intra bony periodontal defects<sup>[5]</sup>. Moreover, coated nHA implants in rabbits' femur demonstrated better implant and bone contact than uncoated samples<sup>[12]</sup>. Also, enhanced bone formation was detected in nHA lining Poly lactic co-glycolic acid (PLGA) scaffolds in defects of rabbits<sup>[13]</sup>. Another study noted intensified spreading and proliferation of alveolar osteoblasts from 4 to 14 days when grown up on culture plates lined with nHA<sup>[14]</sup>.

Favorable osteogenic capacity and enhancement of bone regeneration of nHA were explained as the nano-sized particles and their structural similarity to natural bone allow HA nanocrystals to bond firmly to bone. This stimulates the proliferation and metabolism of osteoblasts permitting better osseointegration and strong osteoconductive and osteoinductive ability<sup>[12]</sup>. It was suggested that when nHA starts to dissolve, it releases calcium ions in the surrounding environment which encourages cell proliferation and osteogenic differentiation. The authors added that nHA can augment mineral deposition promoting rapid neo-osteogenesis<sup>[15]</sup>. It was speculated that if HA was placed underneath healthy periosteum and properly vascularized bone, it will release phosphate ions into the medium inducing bone healing<sup>[14]</sup>. The authors proposed that nHA induces alveolar osteoblasts to secrete specific bone morphogenic proteins (BMPs) and other growth factors which stimulate and regulate bone regeneration process<sup>[14]</sup>.

The Biodentine group showed evidence of granulation tissue, collagen bundles and inflammatory cells infiltration in one and two week's post-surgical durations. These observations are in agreement with others who demonstrated moderate inflammatory reaction in subcutaneous tissue of rats treated with Biodentine. They also recorded a significant increase in fibroblasts and collagen bundles synthesis. The inflammatory reaction of Biodentine may be attributed to its chemical components<sup>[16]</sup>.

Present results revealed more bony spicules with widened lacunae in the two weeks Biodentine group. Osteoblast-like cells were obvious in the vicinity of the newly formed trabeculae. Other investigators confirmed osteoblast-like cells attachment and proliferation on the surface of Biodentine within 5 days incubation period in vitro<sup>[17]</sup>. Similar outcome was reviewed regarding the material's in vitro effect over a period of 20 days revealing significant increase in human osteoblastic cell concentration<sup>[7]</sup>.

It was proposed that Biodentine constituents of calcium silicate, carbonate and zirconium oxide are markedly biocompatible, displaying high osteogenic potential and promoting bone neof ormation as well<sup>[16&18]</sup>. Biodentine was suggested to increase osteoblast-like cell differentiation by enhancing their proliferation and attachment. These cellular actions may be related to the nano-features and topography of the material<sup>[17]</sup>, which allows large surface area for protein adsorption<sup>[19]</sup>. In addition, bone regeneration starts when osteogenic signals unite with soluble molecular signals such as calcium which triggers cascade of cellular differentiation into osteoblast cell lines resulting in bone matrix formation<sup>[19]</sup>. Another hypothesis suggested that calcium silicate cements show alkaline pH and are able to release calcium ions<sup>[20]</sup>. These conditions induce nucleation of calcium phosphates and apatite which favor osteoblastic activity and mineralization process<sup>[21]</sup>.

Furthermore, some investigations could be interpreted supporting that Biodentine stimulates the release of transforming growth factor  $\beta$ 1 (TGF- $\beta$ 1) from pulp cells. This may result in activation of odontoblastic differentiation together with mineralization in the form of osteodentin<sup>[22]</sup>. Further studies subjected Saos-2 cells (a model for osteoblastic cells) to Biodentine in vitro. Data confirmed elevated expression of bone morphogenetic protein-2 (BMP-2) encouraging osteogenic differentiation and formation of mineralizing nodules<sup>[23]</sup>.

Runx- 2 is a chief transcription factor for osteoblastic differentiation, matrix formation, and mineralization throughout bone synthesis<sup>[24]</sup>. This essential gene is required for induction of osteoblasts; hence, bone regeneration process as the regulation of differentiation of osteoblasts by Runx- 2 occurs during initial stages of differentiation, whereas it inhibits this process in advanced stages<sup>[25]</sup>. Statistical analysis of Runx- 2 gene expression revealed significant increase in both Biodentine and Nano Bone

groups compared to control group throughout the three experimental periods (3days, 1 week, 2 weeks). Similar results of elevated levels of Runx- 2 gene expression were detected in vitro<sup>[26]</sup> showing high osteogenic differentiation potency of icariin (a herbal treatment of osteoporosis). The increase in Runx- 2 expression levels reflects the elevated bone regeneration activity. Furthermore, Nano Bone grafted defects created at the upper and lower first premolars in dogs demonstrated the existence of Runx-2-positive osteoblast precursor cells at the treated sites<sup>[27]</sup>.

On the other hand, collagen 1 alpha is a specific osteogenic protein and transcription factor that indicates osteogenic differentiation<sup>[28]</sup>. In the ongoing study, statistical analysis of collagen 1 alpha gene expression revealed a significant increase in the treated groups after 3 days, 1 week and 2 weeks when compared to the control. In this regard, both collagen 1 alpha and Runx- 2 genes were used as osteogenic markers for human bone marrow stem cells (hBMSCs) in vitro<sup>[29]</sup>. Expression levels of collagen 1 alpha and Runx- 2 genes were obviously increased in SIRT7 down regulated hBMSCs than in the control group at 3 and 7 days presenting increased osteogenic activity. Another study documented that adding Nell-1, a bone regeneration growth factor, on the surface of titanium disks revealed significant raise of collagen 1 alpha and Runx- 2 genes levels after 6 days promoting pre-osteoblasts differentiation<sup>[30]</sup>.

## CONCLUSION

From the fore mentioned information it can be concluded that both Nano Bone and Biodentine had proven their osteogenic capability. Though Biodentine had initiated osteogenesis in the herein study; yet the newly formed bone was of lesser quality than Nano Bone as observed histologically. Furthermore, unexpected reactions including intense inflammation were detected through numerous inflammatory cells infiltration during one and two week's experimental periods. In addition, fatty degeneration was documented particularly at one week interval. Statistical analysis confirmed these results as Runx- 2 showed significant increase in Nano Bone group compared to Biodentine group at 1 week, while collagen1 alpha gene expression was significantly increased throughout the three intervals. This could be attributed to the nature of the tissue to which the material was applied; being regularly used with dentin rather than bone.

Nevertheless, further investigation is needed; particularly concerning Biodentine regarding its effect on periodontal tissues that are in intimate relation to treated teeth with the material as in cases involving root fracture and discover the results of the long term follow up.

## CONFLICTS OF INTEREST

There are no conflicts of interest.

## ABBREVIATIONS

- Nano Bone (Artoss, Rostock Comp. Germany).

- Biodentine™ (Active Biosilicate Technology SEPTODONT, France).
- Ketamine ®, Amoun CO.
- Xyla-Ject®, Phoenix™, Pharmaceutical Inc.
- Pentabiotic Veterinário Pequeno Porte, Fort Dodge®

## REFERENCES

1. Jahangirnezhad M, Kazeminezhad I, Saki G, Amirpoor S and Larki M: The effects of Nanohydroxyapatite on bone regeneration in rat calvarial defects. *Am. J. Res. Com.* (2013) 1(4): 302-316.
2. Zhou H and Lee J: Nanoscale hydroxyapatite particles for bone tissue engineering. *Acta. Biomater.* (2011) 7(7): 2769-2781.
3. Liu Q, Douglas T, Zamponi C, Becker ST, Sherry E, Sivanathan S, Warnke F, Wiltfang J and Warnke PH: Comparison of in vitro biocompatibility of NanoBone® and BioOss® for human osteoblasts. *Clin. Oral Implants Res.* (2011) 22(11):1259-1264.
4. Canullo L, Dellavia C and Heinemann F: Maxillary sinus floor augmentation using a nano-crystalline hydroxyapatite silica gel: case series and 3-month preliminary histological results. *Ann. Anat.* (2012) 194(2):174-178.
5. Heinz B, Kasaj A, Teich M and Jepsen S: Clinical effects of nanocrystalline hydroxyapatite paste in the treatment of intrabony periodontal defects: a randomized controlled clinical study. *Clin. Oral Invest.* (2010) 14(5):525-531.
6. Sindhura A, Arun A and Shashikala K: Platelet Rich Fibrin (PRF) with Biodentine - A Novel Approach for Bone Augmentation in Infected Periapical Cyst: Case Reports. *International Journal of Health Sciences and Research.* (2015) 5(11):371-379.
7. Rajendran M, JeevaRekha M and Poorana, K: Biodentine: Periodontal perspective. *International Journal of Applied Dental Sciences.* (2017) 3(1):12-16.
8. Atalay Y, Bozkart M, Gonul Y, Cakmak O, Agacayak KS, Köse I, Hazman O, Keles H, Turamanlar O and Eroglu M: The effects of amlodipine and platelet rich plasma on bone healing in rats. *Drug Des. Devel. Ther. Apr.* (2015) 9: 1973-1981.
9. Lim J, Lee J, Yun H, Shin H and Park E: Comparison of bone regeneration rate in flat and long bone defects: Calvarial and tibial bone. *Tissue Engineering and Regenerative Medicine.* (2013) 10(6):336-340.
10. Chan Y: Biostatistics102: Quantitative Data – Parametric and Non-parametric Tests. *Singapore Med J.* (2003) 44(8):391-396.
11. Scarano A, Perrotti V, Degidi M, Piattelli A and Iezzi G: Bone regeneration with algae-derived hydroxyapatite: a pilot histologic and morphometric study in rabbit tibia defects. *Int. J. Oral Maxillofac. Implants.* (2012) 27(2):336-340.

12. Barkarmo S, Wennerberg A, Hoffman M, Kjellin P, Breiding K, Handa P and Stenport V: Nano-hydroxyapatite-coated PEEK implants. A pilot study in rabbit bone. *J Biomed. Mater. Res A.* (2013) 101(2):465-471.
13. Wang D, Hi Y, Bi L, Qu ZH, Zou JW, Pan Z, Fan JJ, Chen L, Dong X, Liu XN, Pei GX and Ding JD: Enhancing the bioactivity of Poly (lactic-co-glycolic acid) scaffold with a nano-hydroxyapatite coating for the treatment of segmental bone defect in a rabbit model. *Int J Nanomedicine.* May (2013) 8:1855-1865. doi: 10.2147/IJN.S43706.
14. Pilloni A, Pompa G, Saccucci M, Di Carlo G, Rimondini L, Brama M, Zeza B, Wannenes F and Migliaccio S: Analysis of human alveolar osteoblast behavior on a nano-hydroxyapatite substrate: an in vitro study. *BMC Oral Health.* Mar. (2014) 14:22. doi: 10.1186/1472-6831-14-22.
15. Jianzhong H, Yongchun Z, Lihua H, Jun L and Hongbin L: Effect of nanohydroxyapatite coating on the osteoinductivity of porous biphasic calcium phosphate ceramics. *BMC Musculoskelet. Disord.* Apr. (2014) 15:114. doi: 10.1186/1471-2474-15-114.
16. da Fonseca, T, Silva G, Guerreiro-Tanomaru J, Delfino M, Sasso-Cerri E, Tanomaru-Filho M and Cerri P: Biodentine and MTA modulate immunoinflammatory response favoring bone formation in sealing of furcation perforations in rat molars. *Clin. Oral Investig.* (2019) 23(3):1237-1252.
17. Attik G, Villat C, Hallay F, Pradelle-Plasse N, Bonnet H, Moreau K, Colon P and Grosgeat B: In vitro biocompatibility of a dentine substitute cement on human MG63 osteoblasts cells: Biodentine™ versus MTA. *Int Endod J.* (2014) 47(12):1133-1141.
18. Gandolfi M, Iezzi G, Piattelli A, Prati C and Scarano A: Osteoinductive potential and bone-bonding ability of ProRoot MTA, MTA Plus and Biodentine in rabbit intramedullary model: Microchemical characterization and histological analysis. *Dent Mater.* (2017) 33(5):e221-e238.
19. Chen G, Deng G and Li Y: TGF- $\beta$  and BMP signaling in osteoblasts differentiation and bone formation. *Int. J. Biol. Sci.* (2012) 8(2):272-288.
20. Lucas C, Viapiana R, Bosso-Martelo R, Guerreiro-Tanomaru J, Camilleri J and Tanomaru-Filho M: Physicochemical properties and dentin bond strength of a tricalcium silicate-based retrograde material. *Braz. Dent. J.* (2017) 28(1):51-56.
21. Prati C and Gandolfi M: Calcium silicate bioactive cements: biological perspectives and clinical applications. *Dent. Mater.* (2015) 31(4):351-370.
22. Priyalakshmi S and Ranjan M: Review on Biodentine- A Bioactive Dentine Substitute. *IOSR Journal of Dental and Medical Sciences.* (2014) 13(1):13-17.
23. Rodrigues E, Gomes-Cornélio A, Soares-Costa A, Salles LP, Velayutham M, Rossa-Junior C, Guerreiro-Tanomaru JM and Tanomaru-Filho M: An assessment of the overexpression of BMP-2 in transfected human osteoblast cells stimulated by mineral trioxide aggregate and Biodentine. *Int Endod J. Dec.* (2017) 50Suppl 2:e9-e18.
24. Lu SL, Su PY, Li CL, Wang LF and Lu HK: Regulation of pre-osteoblast osteogenic transcription factors by different titanium surface topography. *J Dent Health Oral Disord. Ther. Sep.* (2017) 8(2): 00278 doi:10.15406/jdhodt.2017.08.00278.
25. Jiahai X, Zhanghua L, Yudong H and Weijun F: Potential mechanisms underlying the Runx2 induced osteogenesis of bone marrow mesenchymal stem cells. *Am. J. Transl. Res.* (2015) 7(12):2527-2535.
26. Ma HP, Ma XN, Ge BF, Zhen P, Zhou J, Gao YH, Xian CJ and Chen KM: Icariin attenuates hypoxia-induced oxidative stress and apoptosis in osteoblasts and preserves their osteogenic differentiation potential in vitro. *Cell Prolif.* (2014) 47(6), 527-539.
27. Seifi M, Arayesh A, Shamloo N and Hamed R: Effect of nanocrystalline hydroxyapatite socket preservation on orthodontically induced inflammatory root resorption. *Cell Journal (Yakhteh).* (2015) 16 (4): 514-527.
28. Uchihashi K, Aoki S, Matsunobu A and Toda S: Osteoblast migration into type I collagen gel and differentiation to osteocyte-like cells within a self-produced mineralized matrix: a novel system for analyzing differentiation from osteoblast to osteocyte. *Bone.* (2013) 52 (1):102-110.
29. Chen EM, Zhang W, CY Ye C, Gao X, Jiang LL, Zhao TT, Pan ZZ and Xue DD: Knockdown of SIRT7 enhances the osteogenic differentiation of human bone marrow mesenchymal stem cells partly via activation of the Wnt/ $\beta$ -catenin signaling pathway. *Cell Death and Dis. Sep.* (2017) 8(9), e3042. doi: 10.1038/cddis.2017.429.
30. Shen M, Wang G, Wang Y, Xie J and Ding X: Nell-1 Enhances Osteogenic Differentiation of Pre-Osteoblasts on Titanium Surfaces via the MAPK-ERK Signaling Pathway. *Cell Physiol. Biochem.* (2018) 50(4): 1522-1534.

## التحفيز على تكوين العظام وقدرة شفاء العظام لمادة هيدروكسيباتيت النانوي البلوري مقابل مادة البيودنتين فى التجويفات الجراحية للعظم السنخي للأرانب (دراسة فى الحيوان)

هبة محمد حكم<sup>١</sup>، رحاب على عبد المنعم<sup>١،٢</sup>، منى الديب<sup>٢</sup>

<sup>١</sup>بيولوجيا الفم كلية طب الأسنان جامعة القاهرة.

<sup>٢</sup>قسم بيولوجيا الفم كلية طب الفم والأسنان جامعة المستقبل

**مقدمة:** يعتبر التجويف العظمى الناتج عن الصدمات واستئصال الأورام والعدوى والتشوهات الخلقية والمكتسبة من المشاكل المرضية الأساسية. لقد استخدمت المادة المصنعة هيدروكسيباتيت النانوي البلوري بنجاح فى علاج تجويفات العظام بدون ملاحظة أى اثار جانبية سلبية. كما ان مادة البيودنتين المصنعة اساسا من مادة سيليكات الكالسيوم تعتبر مادة مكونة للعظم والأوعية الدموية. **الأهداف:** تهدف هذه الدراسة الى بحث المقدرة الأولية لمادتي هيدروكسيباتيت النانوي البلوري البيودنتين للتحفيز على تكوين العظام فى التجويفات الجراحية للعظم السنخي للأرانب.

**طريقة البحث والمواد المستخدمة:** تمت هذه الدراسة على عدد 30 ذكر من الأرانب البالغة. تم عمل تجويف جراحى على جانبى الفك السفلى لجميع الأرانب: وقد أعتبر الجانب الأيمن هو الجانب التجريبي بينما الجانب الأيسر ترك فارغا للمراقبة. تم تقسيم الأرانب عشوائيا الى مجموعتين بكل منهما عدد 15 أرنب: المجموعة الأولى (البيودنتين) حيث تم وضع مادة البيودنتين فى الجانب الأيمن من الفك السفلى. المجموعة الثانية (هيدروكسيباتيت النانوي البلوري) حيث تم وضع المادة فى الجانب الأيمن من الفك السفلى للحيوانات. استخدم الموت الرحيم لعدد 5 أرانب من كل مجموعة على فترات وهى: 3, 7, 14 يوم عقب العملية الجراحية. تم تجهيز العينات بعد ذلك للفحص النسيجي باستخدام المجهر الضوئى وكذلك التحليل الكمي للتعبير الجيني للكولاجين و Runx-2 باستخدام تفاعل البلمرة المتسلسل.

**النتائج:** مادة البيودنتين لها مقدرة على بدء تكوين العظم ولكن نوعية العظم الحديث تعتبر أقل من العظم المكون من مادة الهيدروكسيباتيت النانوي البلوري. وقد أظهرت نتائج Runx-2 زيادة واضحة فى مادة الهيدروكسيباتيت النانوي البلوري بالمقارنة بمادة البيودنتين بعد أسبوع من التجربة. أما التحليل الكمي للتعبير الجيني للكولاجين فقد أظهر زيادة واضحة فى جميع فترات التجربة.

**الخلاصة:** كلتا المادتين الهيدروكسيباتيت النانوي البلوري والبيودنتين لديهما المقدرة على بدء تكوين العظم ولكن مادة الهيدروكسيباتيت النانوي البلوري أظهرت نتائج شفائية أفضل من مادة البيودنتين.